Journal of Applied Polymer Science

In Situ Synthesis of Nano Silver on Polyester Using NaOH/Nano TiO_2

Vida Allahyarzadeh,[1] Majid Montazer,[1] Nahid Hemmati Nejad,[1] Nasrin Samadi[2]

[1]Textile Engineering Department, Center of Excellence in Textile, Amirkabir University of Technology, Tehran, Iran

[2]Department of Drug and Food Control, Faculty of Pharmacy and Pharmaceuticals Quality Assurance Research Center, Tehran University of Medical Sciences, Tehran, Iran

Correspondence to: M. Montazer (E-mail: tex5mm@aut.ac.ir)

ABSTRACT: Alkali hydrolysis of polyester along with application of nano silver/nano TiO_2 to produce hydrolyzed polyester fabric with antibacterial and self-cleaning properties is a very interesting subject. In this article, a novel idea is introduced to achieve a polyester fabric with self-cleaning and antibacterial properties with a good feeling handle in one step. The polyester fabric is hydrolyzed in alkali media to enhance the surface activity, improve nanoparticle absorption, and produce ethylene glycol for reducing silver nitrate into nano silver. XRD pattern confirms the presence of nanoparticles with crystal size of 10 nm on the fabric surface and FESEM pictures show the distribution of nanocomposite particles on the fiber surfaces with average size of 54 nm. The degradation of Methylene Blue under daylight irradiation confirms the photoactivity of nano TiO_2 on the polyester fabric. Also, very good bactericidal efficiency is obtained against *S. aureus* and *E. coli*. Interestingly, the fabric tensile strength improves even with the action of alkali in surface hydrolysis of polyester. © 2013 Wiley Periodicals, Inc. J. Appl. Polym. Sci. 129: 892–900, 2013

KEYWORDS: polyester; alkali hydrolysis; nano silver; nano TiO_2; antibacterial; self-cleaning

Received 5 August 2012; accepted 5 December 2012; published online 3 January 2013
DOI: 10.1002/app.38907

INTRODUCTION

Over the past decade, alkaline hydrolysis of polyester (PET) fabric has been used to improve the physical properties of PET fabrics. This type of finishing process leads to controlled degradation of surface fabric and produces desirable properties on PET fabrics.[1,2] The chain cleavage happens with alkaline hydrolysis of PET by sodium hydroxide in two ways: unimolecular and bimolecular cleavage, in which a single hydroxide ion and two hydroxide ions react with polymer chain, respectively. The polymer by progressive reaction of chain with hydroxide ion is hydrolyzed to monomer units and alternately removed terephthalate anions and ethylene glycol.[3]

Silver nanoparticles have attracted much attention because of distinctive properties, such as good conductivity, chemical stability, and catalytic and antibacterial activities. Numerous synthesis approaches have been developed to obtain silver nanoparticles including chemical reduction, photochemical, polysaccharide, Tollen's reagent, UV irradiation, biological and polyoxometalates methods.[4–16] Also, ethylene glycol has been used as a reducing agent in the synthesis of silver nanoparticles[17,18] acting as a media in the preparation of the metal oxides via hydrolysis of metal salts.[19–25] Further, silver nanoparticles were synthesized by either heating the precursor solution to the reaction temperature or injecting an aqueous silver salt solution into hot ethylene glycol.[26] The silver nanoparticles were also synthesized by ethylene glycol and glucose as reducing agent and also poly [*N*-vinylpyrolidone] (PVP) as a stabilizer.[27] Also, the radiolysis of Ag^+ ions in ethylene glycol has been applied to synthesize silver nanoparticles.[28] Furthermore, Ag nanoparticles with different size were synthesized successfully by using microwave-polyol method.[29]

Many synthesis methods have been employed for silver nanoparticles production in alkali media through reduction of $[Ag(NH_3)_2]^+$ with monosaccharides and disaccharides at pH conditions 11.5–13.0.[30] Additionally, with $NaBH_4$ in alkaline aqueous solutions silver nanoparticles were supported on halloysite nanotubes (Ag/HNTs).[31] Also, gold, silver, and gold–silver alloy nanoparticles were capped with decanethiolate monolayer shells synthesized in alkali media.[32] Synthesis of silver nanoparticles using enzyme under alkaline conditions has also been reported.[33]

In recent years, nano titanium dioxide (TiO_2) has many applications because of higher stability, long lasting, safe and broad-spectrum antibiosis, their photocatalytic activity, and ability to absorb ultraviolet irradiation.[34] Also, synthesis of Ag nanoparticles on the surface of TiO_2 has attracted some attention due to the synergistic effect of Ag/TiO_2 nanocomposite. The

desirable antibacterial wool fabric has been prepared by synthesis of Ag/TiO_2 nanocomposite on the surface of wool fabric.[35] Further, Ag/TiO_2 nanocomposites and PVA-capped colloidal Ag/TiO_2 nanocomposites have been prepared.[36] The electron exchange between Ag and TiO_2 leads to a red shift Plasmon peak appearing as a brownish color on the treated textiles, which can be overcome by application of silver and TiO_2 nanoparticles in two steps separately and stabilized with cross-linkable polysiloxane (XPs).[37,38]

Likewise, it is known that the stability of nanoparticles on PET is low because of lack of functional groups.[39] It is necessary to create some functional groups on the polyester polymeric chains. Also, chemical surface modification such as alkali hydrolysis increases the functionality of polyester fibers by introducing hydroxyl and, particularly, carboxylic groups onto the surface of fabric imparting new specifications to the fabric, such as better binding to nano-TiO_2 particles.[40–45]

In the present work, *in situ* synthesis of silver nanoparticles along with application of TiO_2 nanoparticles in alkali media has been considered to achieve multifunctional PET fabric with diverse properties such as antimicrobial activity, self-cleaning, and good hand feeling. This offers a simultaneous alkali hydrolysis of polyester fabric with synthesis of nano silver and application of nano TiO_2 on the polyester fabric reducing the finishing processing steps. In addition, the properties of treated PET fabric such as antimicrobial activity, self-cleaning, wettability, tensile strength, and bending length have been studied and reported.

EXPERIMENTAL

Material

The plain, white PET fabric with 188.5 g/m^2 and 150 Den filaments (Nafis Yarn Co., Iran), silver nitrate ($AgNO_3$, extra pure >99.8%, Merck, Germany), sodium hydroxide (Merck, Germany), cetyl trimethyl ammonium bromide (Darmstadt, Germany), and nano-TiO_2 (21 nm, Degussa P25, Evonik, Germany) were used.

Pretreatment of PET Fabrics

To clean the PET fabrics from the impurities, the samples were washed in a solution containing 2 g/L nonionic detergent for 30 min at 60°C with liquor to goods ratio($L : G$) of 40 : 1, then rinsed with distilled water and dried at ambient temperature.

In Situ Synthesis of Ag Nanoparticles and Application of TiO_2 Nanoparticles

The fabric samples were finally cut into suitable pieces, weighed, and then were put in the bath with $L : G = 40 : 1$ along with other materials (Table I) and boiled for 1 h. The treated samples were rinsed with distilled water and dried at room temperature.

Test Methods

The weight loss percentage (WL %) of each sample was determined according to eq. (1):

$$\mathrm{WL}\% = \frac{W_1 - W_2}{W_1} \times 100 \quad (1)$$

where W_1 and W_2 are the weights of the samples before and after treatment, respectively.

Table I. Preparation of Different Samples

Sample code	NaOH (w/v %)	$AgNO_3$ (w/w %)	CTAB (w/w %)	Nano TiO_2 (w/w %)
S1	0.5	-	-	-
S2	0.5	0.003	-	-
S3	0.5	-	0.1	-
S4	0.5	-	-	0.5
S5	0.5	0.003	0.1	-
S6	0.5	0.003	-	0.5
S7	0.5	-	0.1	0.5
S8	0.5	0.003	0.1	0.5

A Nicolet FTIR was employed by taking the spectra between 400 and 4000 cm^{-1} for analysis of the changes appeared in functional groups on fabrics surface through the chemical treatment.

Also, X-ray diffraction (XRD, model EQuniox3000, INEL, France) with nickel-filtered Cu Kα radiation was used to study the presence and crystalline structure of the absorbed nanoparticles on the fabric surface and to estimate the size of crystalline structure. The crystalline size was calculated through Scherrer's eq. (2):

$$D = \frac{K\lambda}{B_{\mathrm{cor}} \cos\theta_B}, \qquad \mathrm{B_{cor}} = (\mathrm{B^2}_{\mathrm{sample}} - \mathrm{B_2}^{\mathrm{ref}})^{1/2} \quad (2)$$

where D is the average crystal size, K is the Scherrer coefficient (0.9), λ is the X-ray wavelength (λ = 1.540560 Å), θ is the Bragg's angle, B_{cor} is the corrected full width at half-maximum (FWHM) in radians, and B_{sample} and B_{ref} are the FWHM of the reference and sample peaks, respectively.[46]

Additionally, the degradation activity of 0.005% w/v Methylene Blue was evaluated by daylight irradiation of the treated samples for 10 h to investigate the self-cleaning properties of the fabrics. The color change of the fabrics was evaluated using image processing in which the color difference in RGB color space was calculated according to eq. (3):

$$\Delta\mathrm{RGB} = ((B_2 - B_1)^2 + (G_2 - G_1)^2 + (R_2 - R_1)^2)^{1/2} \quad (3)$$

The higher ΔRGB value corresponds to the higher self-cleaning properties.

Further, quantitative antibacterial efficiency of the treated fabrics was determined against *Staphylococcus aureus* ATCC 6538 as a Gram-positive and *Escherichia coli* ATCC 8739 as Gram-negative bacteria according to AATCC test method 100-2004. The circular samples (4.8 ± 0.1 cm) were individually placed in a sterile 250 mL beaker and inoculated with 1 mL bacterial suspension (10^7 CFU/mL). After proper exposure time (0 and 6 h), 100 mL neutralizing solution (sodium thiosulphate ($Na_2S_2O_3$) 1% and Tween 80, 0.1% (w/v)) was added to inoculated samples to neutralize microbial growth and stirred

for 15 min at 25°C. The antibacterial efficiency of the treated fabrics as term of bactericidal was calculated by eq. (4):

$$K\%\ (\text{bactericidal efficiency}) = \frac{A-B}{A} \times 100 \qquad (4)$$

where A is the number of bacteria recovered from the unloaded test specimen (control sample) at 0 contact time and B is the number of bacteria recovered from the loaded wool sample with Ag nanoparticles at 6 h contact time.

The hydrophilicity of the fabrics was studied by measuring the time required for the water droplet to adsorb and spread on the fabric surfaces according to AATCC Test Method 79-2000. To this end, a drop of distilled water was dropped from 1 cm on the fabric surface by a small syringe. The time of the complete adsorption of water droplets on the fabric surfaces was measured for 10 replicates, and the average value was reported.

Also, to evaluate the effect of treatment on the mechanical properties of the treated fabrics, the tensile strength was tested by using Instron with gauge length of 5 cm and extension rate of 200 mm/min for three replicates, and the average value was recorded.

Field emission scanning electron microscopy (FESEM) (Hitachi S4160) was used to observe fabric surfaces. Energy-dispersive X-ray (EDX) mode was applied for elemental composition analysis. A gold layer was deposited on the fabrics before analysis.

Moreover, the effect of treatment on the hand feeling of the treated samples was characterized by the bending length of samples using Shirley bending length tester (Shirley, UK). The bending rigidity of samples was calculated according to BS: 3356, 1990 using eq. (5):

$$B_{FAST} = W.c^3.(9.807).10^{-6} \qquad (5)$$

where W is the area density in g/m^2 and c = l/2 in mm is the bending length of samples.[47]

RESULTS AND DISCUSSION

Weight Loss

The weight loss of the treated fabrics indicated increase in weight loss percentages after alkali treatment (Table II). However, 0.5% NaOH was used as a low concentration with the low weight loss.

It is well known that the alkaline hydrolysis of PET fabrics with sodium hydroxide is topochemical degradation. This takes place at the fiber surfaces and caused polyester chains cleavage of the surface, decreased fiber diameter while showing pits and holes on fiber surfaces. During polyester hydrolysis by alkali metal hydroxides, the hydroxide ions attack the electron-deficient carbonyl resulting in hydroxyl (—OH) and carboxyl (—COOH) end groups production at the fiber surfaces removing the low molecular segment of the chains decreasing fabric weight and fiber diameter. Prolonged treatment time with increased sodium hydroxide concentration leads to the higher WL%.[48]

Table II. Different Properties of Treated Polyester Fabrics

Sample code	Weight loss (%)	ΔRGB	B_{FAST} (μNm)
S1	0.77	10.2	17.12
S2	0.65	18.9	9.08
S3	0.95	31.2	12.68
S4	0.4	22.2	9.08
S5	1.05	35.6	12.68
S6	0.65	33.4	19.68
S7	1.00	37.8	12.68
S8	0.95	44.4	15.93

Additionally, WL% of the fabrics treated with NaOH and cetyl trimethyl ammonium bromide (CTAB) (samples S3, S5, S7, and S8) were higher than fabrics treated without CTAB. CTAB as a cationic surfactant increases the hydrolysis reaction rate due to the ability of long-chain molecules to transfer hydroxide ions into the polyester phase. The induction effect or coverage of negative charges on the hydrolyzed polyester facilitates the next attack of hydroxyl anions.[48,49]

Fourier Transform Infrared Spectroscopy

All of the compounds with covalent bond, organic and mineral, absorb different frequency of electromagnetic radiation in IR region. One of the major applications of FTIR spectroscopy is recognizing functional group of compounds. The absorption band pertaining to each bond is found in little part of region vibration's infrared.[50]

It is well known that the absorption band pertaining to C—H (alkenes, bending vibration), C—H (alkenes, stretching vibration), C—O (ester and carboxylic acid, stretching vibration), C=C (alkenes, stretching vibration), C=O (carboxylic acid, stretching vibration), O—H (hydrogen bond, stretching vibration), and O—H (carboxylic acid, stretching vibration) appear at 1000–650 cm^{-1}, 3100–3000 cm^{-1}, 1300–1000 cm^{-1}, 1680–1600 cm^{-1}, 1725–1700 cm^{-1}, 3500–3200 cm^{-1}, and 3400–2400 cm^{-1}, respectively.[50]

The infrared spectrum of raw polyester (Figure 1) shows the characteristic peaks attributed to C=O (carboxylic acid), C—O (ester and carboxylic acid), C—H (bending vibration), and C—H (stretching vibration) at 1716, 1240 and 1097, 2967, and 730 cm^{-1}, respectively. After alkaline hydrolysis (sample S1), the intensity of characteristic peaks ascribed to —OH at 3054 and 3419 cm^{-1} and the peak attributed to C=O (carboxylic acid) at 1716 cm^{-1} was increased, but no change was detected at other peaks. This proves the production of hydroxyl (—OH) and carboxyl (—COOH) functional groups on the fiber surface as a result of alkaline hydrolysis. The intensities of the peaks ascribed to OH and COOH increased for S3 and S4 compared with S1 showing higher formation of hydroxyl and carboxyl functional groups. Also, comparing S2, S5, S6, S7, and S8 with S1 indicated a decrease in the intensity of the peaks ascribed to C=O (carboxylic acid) at 1716 cm^{-1} confirming possible formation of linkage between silver and/or TiO_2 with polymer chains.

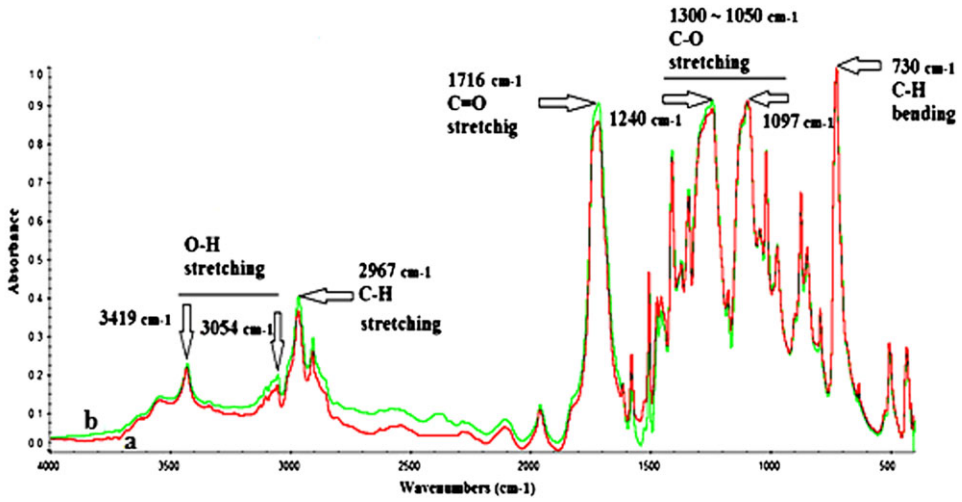

Figure 1. FTIR spectra of PET fabrics: (a) raw PET and (b) alkali-treated PET fabric (S1). [Color figure can be viewed in the online issue, which is available at wileyonlinelibrary.com.]

In sum, presence of different materials has changed the intensities of the peak ascribed to —OH and C=O functional groups.

Synthesis of Nano Silver Particles

In polyol process, ethylene glycol and diols have been used as reducing agents to prepare metal particles. Silver ions in the solution were reduced through the oxidation of hydroxyl groups of poly ethylene glycol to aldehyde groups.[51]

Possible mechanism of *in situ* synthesis of silver nanoparticles during alkaline hydrolysis of polyester fabric is shown in eqs. (6)–(11).[3,9,51] First, the alkaline solution is prepared, and upon the addition of silver nitrate to alkaline solution, the solution became light orange due to the formation of silver oxide (Ag_2O) sediment [eq. (6)]. By increasing the temperature in strong alkaline solution, Ag_2O dissociates into Ag^+ ions [eq. (7)].[52]

In addition, through the alkaline hydrolysis of PET fabrics ethylene glycol was produced. Through the oxidation of hydroxyl groups to aldehyde groups in ethylene glycol, carboxylate ions and e^- were produced. This led to the reduction of silver ions to silver nanoparticles, which resulted in solution discoloration [eqs. (8)–(11)].[3,51]

$$2\ AgNO_3 + 2\ NaOH \rightarrow Ag_2O\ (s) + 2\ NaNO_3 + H_2O\ (l) \quad (6)$$

$$Ag_2O(s) \rightarrow 2Ag^+ + O^{2-} \quad (7)$$

$$\begin{aligned} &H-[-O-CH_2CH_2-O-CO-(C_6H_4)-CO-]_n \\ &-OH + 2\ NaOH \rightarrow HOCH_2CH_2OH + H_2O + \\ &H-[-O-CH_2CH_2-O-CO-(C_6H_4)-CO-]_{n-1} \\ &-OH + NaO-CO-(C_6H_4)-CO-ONa \end{aligned} \quad (8)$$

$$HOCH_2CH_2OH \rightarrow CH_3CHO + H_2O \quad (9)$$

$$CH_3CHO(aq) + 3OH^- \rightarrow CH_3COO^- + 2H_2O + 2e^- \quad (10)$$

$$Ag^+ + e^- \rightarrow Ag^{(0)} \quad (11)$$

Also, FESEM pictures and EDX spectra of sample S2 [Figures 3(b,c) and 4(a)] indicated silver nanoparticles on the fabric surface and confirmed synthesis of silver nanoparticles on the polyester fabric.

Further, the surface charges of TiO_2 nanoparticles in alkaline solution is negative.[53] Therefore, Ag^+ ions bind to $TiO_2^{\delta-}$ by ionic interaction reduced to Ag^0 by e^-. Silver particles in alkaline solution have positive surface charge, thus silver nanoparticles remain on the surface of TiO_2 nanoparticles and Ag/TiO_2 nano composite was produced [eq. (12)].[54]

$$Ag^+ + TiO_2^{\delta-} \rightarrow Ag^+/TiO_2^{\delta-} + e^- \rightarrow Ag/TiO_2 \quad (12)$$

In addition, EDX spectra of sample S8 [Figure 4(b)] showed Ag and Ti elements on the fabric surface and confirmed synthesis of Ag/TiO_2 nanocomposite on the fabric surface.

XRD Patterns

XRD patterns were studied to confirm the presence of nanoparticles on the fabric surface and to estimate their crystalline size.

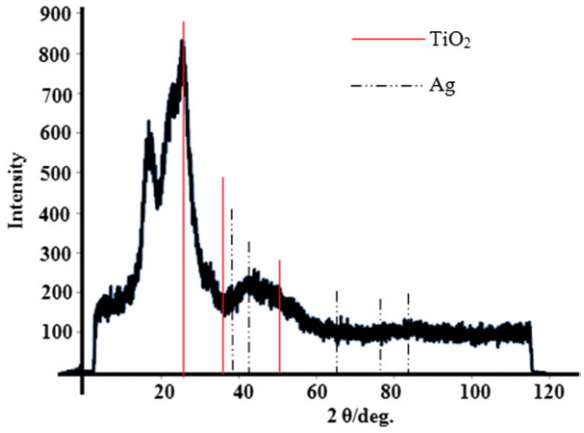

Figure 2. XRD pattern of sample S8. [Color figure can be viewed in the online issue, which is available at wileyonlinelibrary.com.]

Applied Polymer SCIENCE

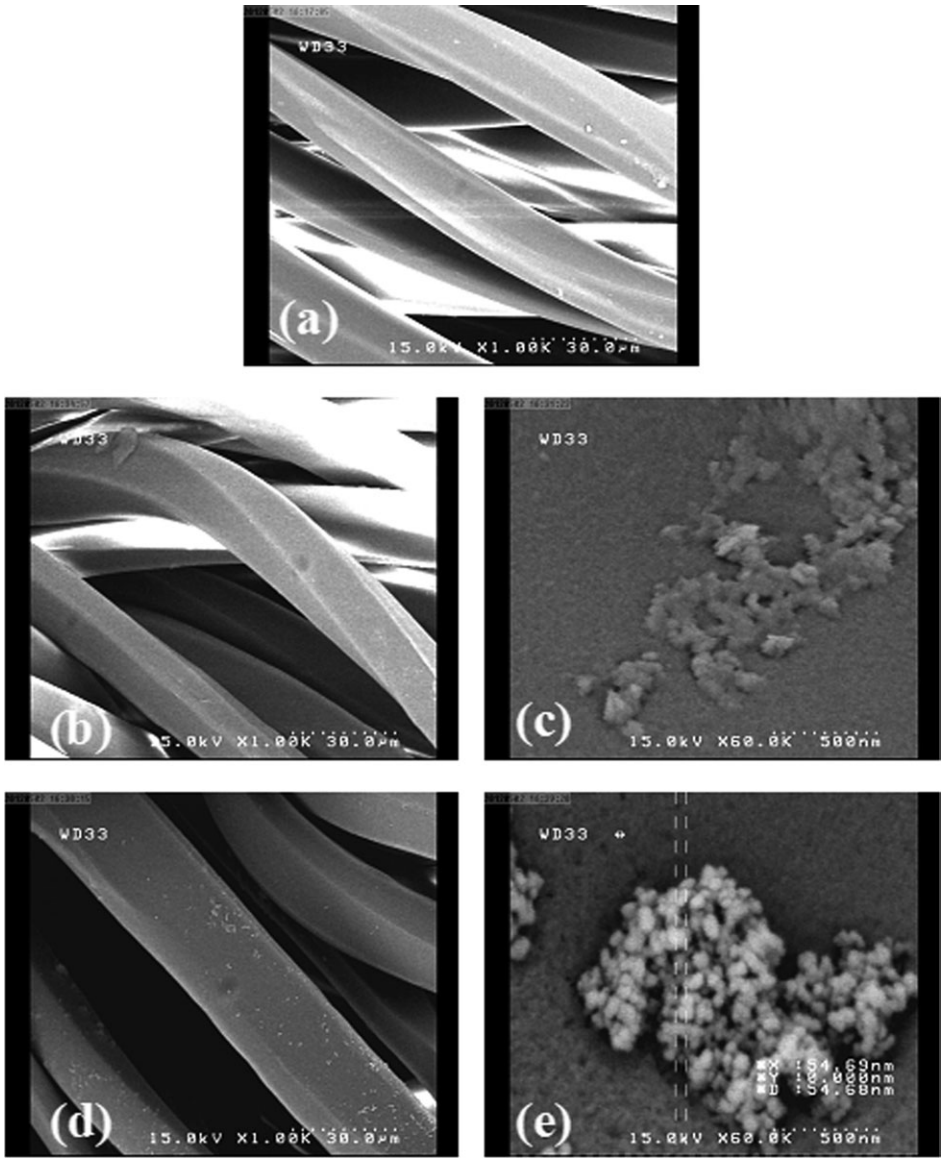

Figure 3. FESEM images of (a) untreated PET fabric, (b) and (c) sample S2 with X60000, and (d) and (e) sample S8 with X60000.

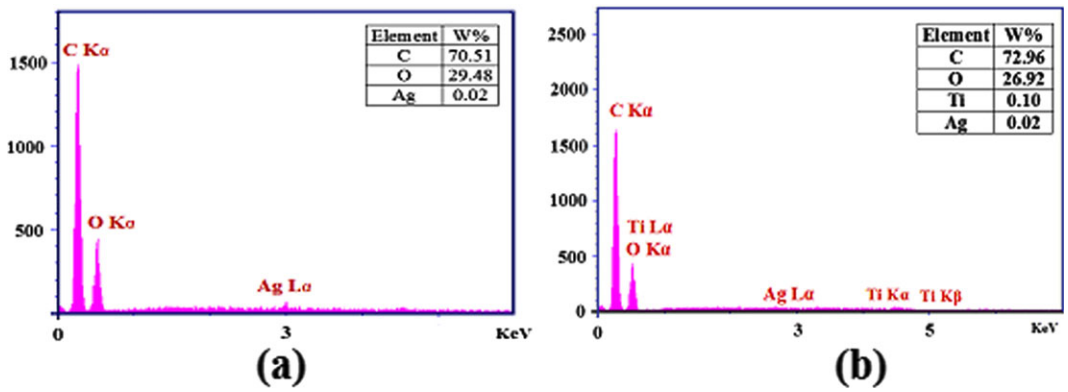

Figure 4. EDX patterns of (a) sample S2 and (b) sample S8. [Color figure can be viewed in the online issue, which is available at wileyonlinelibrary.com.]

The XRD pattern of sample S8 is shown in Figure 2. The peak at 2θ=25.3° confirmed the anatase crystalline phase of TiO_2. It is known that the peaks associated to Ag crystals appeared at 2θ = 38°, 44.5°, and 64° attributed to {111}, {200}, and {220} facets, respectively.[55] The peaks associated to Ag related to sample S8 were not strong due to the low content of synthesized Ag nanoparticles on the polyester fabric surface. However, based on Scherer equation and FWHM data, the crystalline size of all nanoparticles on the polyester fabric surface was about 10 nm. Further, FESEM pictures and EDX spectra of sample S8 (Figures 3 and 4) showed the silver and TiO_2 nanoparticles on the fabric surface and confirmed the above results.

Self-Cleaning Properties

The color change of samples stained with 0.005% Methylene Blue solution was calculated in RGB space and presented in Table II.

Minimum and maximum value of ΔRGB was attributed to samples S1 and S8, respectively, showed no self-cleaning properties on sample S1 and reasonable self-cleaning properties on sample S8. However, samples S4, S6, S7, and S8 treated with nano TiO_2 indicated good self-cleaning properties.

Irradiation by light with more energy of titanium dioxide band gaps generates electron–hole pairs on the surface of the titanium dioxide. The created negative electrons and the positive electric holes combine into oxygen and water and generate O_2^- and hydroxyl radicals, respectively, causing photocatalytic properties of titanium dioxide. Addition of metal ions on the TiO_2 surface can improve the photocatalytic activity of the TiO_2 because of slow coupling of electron and hole.[56] Self-cleaning property of sample S6 was higher than S4 confirmed by higher ΔRGB value.

Additionally, samples S3, S5, S7, and S8 treated with cetyl trimethyl ammonium bromide (CTAB) were indicated by higher ΔRGB values compared with other samples. This phenomenon can be explained by influence of CTAB on the fabric surface in the alkaline process of the PET fabric, which increased the alkaline hydrolysis and produced more hydroxyl groups on the fabric surface. This increases the tendency of fabric surface toward cationic compound such as Methylene Blue. This reduced the local concentration of Methylene Blue on the fabric surface, degraded easily under daylight, and attained higher ΔRGB. Sample S8 showed a maximum photocatalytic activity.

Antibacterial Efficiency

The antibacterial property of treated samples was analyzed against Gram-positive bacteria, *Staphylococcus aureus*, and Gram-negative bacteria, *Escherichia coli*, quantitatively. *S. aureus* is a pathogenic microorganism that causes many diseases such as toxic shock, purulence, abscess, fibrin coagulation, and endocarditis. *E. coli* is commonly found in the lower intestine of warm-blooded organisms (endotherms) and causes gastroenteritis, urinary tract infections, and neonatal meningitis.[57]

The bactericidal efficiencies of the treated fabrics are presented in Table III. For sample S2, *K*% against *S. aureus* and *E.coli* after 6 h contact time was more than 90% and 99%, respectively. This showed that excellent antibacterial property on sample S2 confirmed synthesis of silver nanoparticles through alkaline hydrolysis as indicated by FESEM pictures and EDX patterns.

Table III. Antibacterial Efficiency of Fabric Sample

	K%			
	S. aureus		*E. coli*	
Sample code	0 h contact time	6 h contact time	0 h contact time	6 h contact time
S2	67.7	93.6	42.1	99.8
S3	21.4	99.4	37.8	99.8
S4	58.6	75.7	26.8	95.1
S5	71.4	99.8	35.7	100
S6	75.7	84.3	30.5	100
S7	80.3	100	31.5	99.6
S8	91.4	99.1	22.6	100

Also, the treated fabrics with CTAB including S3, S5, S7, and S8 showed very good antibacterial efficiency against both *S. aureus* and *E.coli* after 6 h contact time. The presence of CTAB in the treatment indicated synergistic effect on the antibacterial efficiency, as the antibacterial property of sample S5 was more than that of sample S2, sample S7 was more than that of sample S4, and sample S8 was more than that of sample S6. Sample S2 loaded with Ag nanoparticles only showed a good antibacterial efficiency against both bacteria. Sample S3 treated with CTAB only indicated a lower antibacterial efficiency in 0 contact time, approximately the same antibacterial efficiency obtained on both samples in 6 h contact time. Sample S5 loaded with Ag nanoparticles and CTAB showed a higher antibacterial efficiency than samples S2 and S3 indicating the synergistic effect of CTAB on the antibacterial efficiency on Ag nanoparticles. Four different reasons can be proposed on this condition. First, presence of CTAB as a catalyst to accelerate alkali hydrolysis led to production of more hydroxyl and carboxyl groups on the fabric surface. This led to more silver and TiO_2 nanoparticles absorption on the fabric surface and consequently increased the antibacterial efficiency of the samples. On the other hand, more ethylene glycol formed due to the more alkali hydrolysis of polyester, producing more silver nanoparticles and Ag/TiO_2 nanocomposite. Also, presence of CTAB in the synthesis of Ag nanoparticles led to formation of small size Ag nanoparticles due to formation of Ag^+/CTAB complex. Thus, Ag^+ ions incorporated with CTAB reduced to Ag^0 by e^-. This reduced the agglomeration of Ag clusters and prevented them from uncontrolled growth. Therefore, Ag nanoparticles with narrow size distribution were produced, which offered higher antibacterial efficiency.[58] Moreover, CTAB is a quaternary ammonium surfactant with effective antiseptic properties against bacteria and fungi.[59] Presence of CTAB in the treatment process indicated synergistic effect on the antibacterial efficiency. All of the mentioned effects influence on the antibacterial efficiency of the treated fabric with CTAB simultaneously. Thus, CTAB played an important role and enhanced the antibacterial properties of the treated fabrics.

Besides, unlike other samples, sample S8 (with Ag/TiO_2 nanocomposite) showed good antibacterial efficiency against *S. aureus* in 0 h contact time.

Wettability

Polyester's hydrophobic nature leads to producing problems, particularly, with regard to soil release and moisture absorption properties in garments. Due to alkaline hydrolysis of PET fabric, the hydrophilicity of fabric was improved.[2] Thus, the water droplets on all of the alkali-modified fabrics were immediate; however, the area of water spreading was different. It was also observed that by using CTAB in the treatment, the area of water droplet spreading on the fabric surface was increased due to enhanced alkaline hydrolysis of polyester fabrics. Increasing alkaline hydrolysis introduces more hydroxyl groups on the fabric surface which led to higher wettability of CTAB-treated fabrics than the others.

Tensile Strength

Although alkaline hydrolysis produced the desirable properties on the PET fabric surface, this led to decrease in tensile strength and fiber diameter causing pitting on the fiber surface that probably worked as nucleation centers for crack formation. By applying tensile load to the alkali-treated polyester fabrics, the pits cause the formation of cracks and then tearing of fabrics.[1] The results confirmed the earlier report as sample S1 (alkali treated) indicated lower tensile strength compared to the raw PET fabric (Table IV). Comparing the maximum breaking load of sample S1 with S3 showed more reduction in presence of CTAB due to higher alkaline hydrolysis. Samples S2, S4, S5, S6, S7, and S8 loaded with nanoparticles (Ag, TiO_2, and Ag/TiO_2) showed higher tensile strain than that of sample S1. Also, sample S8 indicated the highest tensile strength, modulus, and maximum breaking load as the silver nanoparticles were synthesized and nano-TiO_2 was loaded during alkaline hydrolysis on the PET surface. This led to improved tensile strength while the fabric weight was reduced. This phenomenon can be explained by the following reasons:

1. The alkaline hydrolysis has been limited to the surface of fiber in the presence of Ag and TiO_2 nanoparticles creating flatter pits resulted in confining the chain cleavage.
2. The tendency of nanoparticles toward aggregation inside the pits, caused by alkaline hydrolysis, led to filling the pits and smoothing the fiber surface. This caused uniform distribution of load on the fabric surface during tensile measurement delaying the creation and growth of cracks on the fibers surface. Thus, it is more resistant against tensile loading. FESEM picture of sample S8 (Figure 3) showed aggregation of silver and TiO_2 nanoparticles inside pits.
3. Clustering of nanoparticles and their linkages with hydroxyl and carboxyl groups of PET fabric assisted more uniform load distribution during tensile measurement and also delaying the growth of cracks that improved the fabric tensile strength.

Bending Rigidity

The bending rigidity parameters B_{FAST} designed to measure fabric mechanical properties at low-stress level loads and considered as a good factor to indicate the handling characteristic, as an increase in the bending rigidity causes a hard handle.[47] It was further demonstrated that the weight loss of PET fabric could be used as a means of improving their aesthetic properties,[2] as weight loss from 10% to 20% resulted in producing lightweight PET fabrics with silk like properties and imparting hydrophilic properties.[48]

Table IV. Mechanical Properties of Treated Polyester Fabrics

Sample code	Maximum load (N)	Tensile strain (%)	Tenacity (gf/tex)
Raw	417	119	42,529
S1	383	127	39,098
S2	391	128	39,923
S3	380	130	38,777
S4	384	134	39,119
S5	426	138	43,508
S6	429	135	43,704
S7	407	140	41,526
S8	447	131	45,576

The bending rigidity of all the treated samples is presented in Table II. The bending rigidity of nonalkali-treated sample was 32.49 μNm that was reduced to 17.12 μNm with alkali hydrolysis for sample S1. The alkaline treated samples indicated lower bending rigidity, softer handle with more drape. Synthesis of silver nanoparticles along with nano titanium dioxide loading during alkaline hydrolysis of PET fabric (samples S2, S3, S4, S5, S7, and S8) showed lower bending rigidity, resulting in the softer handle. Presence of CTAB in the production of samples S3, S5, S7, and S8 led to increase in the alkaline hydrolysis, which prominently decreased the bending rigidity. Further, presence of TiO_2 along with Ag nanoparticles in sample S6 resulted in higher bending rigidity when compared with sample S2. However, this was reduced by addition of CTAB in sample S8.

FESEM and EDX

FESEM micrographs of the untreated and samples S2, S8 are presented in Figure 3. A smooth uniform surface without any pits can be seen on untreated fabric in Figure 3(a); however, the fiber surface became pitted with holes as reported by others.[2,48] A few pits on the fiber surface can be observed on the fabric treated with low concentration of sodium hydroxide.[2,48] However, presence of silver nanoparticle on the polyester fabric can be confirmed with Figure 3(b,c). This is an evidence for succeeding the proposed method of producing ethylene glycol as reducing agent for reduction of Ag^+ to Ag^0 nanoparticles smaller than 100 nm. The presence of Ag nanoparticles on sample S2 showed in Figure 4(a) with low intensity due to low concentration of Ag and intensive peak ascribed to C and O. Figure 3(d,e) revealed uneven distribution of aggregated Ag/TiO_2 nanoparticles with 54 nm on the fiber surface (sample S8). Also, the presence of Ag and TiO_2 were confirmed by EDX patterns [Figure 4(b)] and revealed the synthesis of Ag/TiO_2 nanocomposite in this method. The nanoparticles aggregated inside

the pits, caused by alkaline hydrolysis, on the fiber surface. Based on the results of FESEM, EDX, and XRD, $AgNO_3$ was reduced to Ag nanoparticles during alkaline hydrolysis.

CONCLUSION

The role of alkaline hydrolysis of polyester fabric in the synthesis of silver nanoparticles was investigated. It is well known that alkaline hydrolysis of polyester fabric with NaOH produces ethylene glycol and functional groups on the polyester chains. The produced ethylene glycol and caboxylate/hydroxyl functional groups can reduce Ag^+ ions to Ag nanoparticles. The presence of TiO_2 led to formation of Ag/TiO_2 nanocomposite and produced white color fabric with reasonable self-cleaning and antibacterial properties offered higher tensile strength. XRD patterns confirmed presence of Ag and TiO_2 nanoparticles on the polyester fabric surface. Further, the treated fabric showed excellent antibacterial properties against *E. coli* and *S. aureus*. Also, the reasonable photoactivity was obtained on the TiO_2 treated polyester fabric by degradation of Methylene Blue as a model compound.

Overall, the proposed method benefits from high efficiencies and environmental friendly behavior that is free from disadvantages involved in conventional Ag nanoparticles synthesis including complicated steps and chemical materials.

REFERENCES

1. East, G. C.; Rahman, M. *Polymer* **1999**, *40*, 2281.
2. Dhinakaran, M.; Dasaradan, B. S.; Subramaniam, V. *J. Text. Apparel Technol. Manage.* **2010**, *6*(3), 1.
3. Latta, B. M. *Text. Res. J.* **1987**, *84*, 766.
4. Sharma, V. K.; Yngard, R. A.; Lin, Y. *Adv. Colloid. Interface Sci.* **2009**, *145*, 83.
5. Vigneshwaran, N.; Nachane, R. P.; Balasubramanya, R. H.; Varadarajan, P. V. *Carbohydr. Res.* **2006**, *341*, 2012.
6. Tai, C.; Wang, Y.-H.; Liu, H.-S. *AIChE J.* **2008**, *54*, 445.
7. Kvítek, L.; Prucek, R.; Panáček, A.; Radko, N.; Hrbac, J.; Zbořil, R. *J. Mater. Chem.* **2005**, *15*, 1099.
8. Panáček, A.; Kvítek, L.; Prucek, R.; Kolár, M.; Večeřová, R.; Pizúrová, N.; Sharma, V. K.; Nevěčná, T.; Zbořil, R. *J. Phys. Chem. B.* **2006**, *110*, 16248.
9. Montazer, M.; Alimohammadi, F.; Shamei, A.; Rahimi, M. K. *Carbohydr. Polym.* **2012**, *87*, 1706.
10. Barani, H.; Montazer, M.; Samadi, N.; Toliyat, T. *Colloids Surf. B* **2012**, *92*, 9.
11. Chen, J.; Wang, W.; Zhang, X.; Jin, Y. *Mater. Chem. Phys.* **2008**, *108*, 421.
12. Mahltig, B.; Gutmann, E.; Reibold, M.; Meyer, D. C.; Bottcher, H. *J. Sol-Gel Sci. Technol.* **2009**, *51*, 204.
13. Shahverdi, A. R.; Minaeian, S.; Shahverdi, H. R.; Jamalifar, H.; Nohi, A. S. *Process Biochem.* **2007**, *42*, 919.
14. Mohan, Y. M.; Mohana Raju, K.; Sambasivudu, K.; Singh, S.; Sreedhar, B. *J. Appl. Polym. Sci.* **2007**, *106*, 3375.
15. Han, K.; Yu, M. *J. Appl. Polym. Sci.* **2006**, *100*, 1588.
16. Li, D.; Haneda, H.; Hishita, S.; Ohashi, N. *Chem. Mater.* **2005**, *17*, 2596.
17. Wiley, B.; Sun, Y. G.; Xia, Y. N. *Acc. Chem. Res.* **2007**, *40*, 1067.
18. Jing, L. Q.; Sun, X. J.; Shang, J.; Cai, W. M.; Xu, Z. L.; Du, Y. G.; Fu, H. G. *Sol. Energy Mater. Sol. Cells* **2003**, *79*, 133.
19. Jezequel, D.; Guenot, J.; Jouini, N.; Fievet, F. *J. Mater. Res.* **1995**, *10*, 77.
20. Collins, I. R.; Taylor, S. E. *J. Mater. Chem.* **1992**, *2*, 1277.
21. Slistan-Grijalva, A.; Gerrera-Urbina, R.; Rivas-Silver, J. F.; Avalos-Borja, M.; Castillon-Barraza, F. F.; Posada-Amarillas, A. *Physica E* **2005**, *25*, 438.
22. Sun, Y.; Mater, B.; Herricks, T.; Xia, Y. *Nano Lett.* **2003**, *3*, 955.
23. Sanguesa, C. D.; Urbina, R. H.; Figlarz, M. *J. Solid State Chem.* **1992**, *100*, 272.
24. LaMer, V. K.; Rober, H. D. *J. Am. Chem. Soc.* **1950**, *72*, 4847.
25. Silvert, P. Y.; Urbina, R. H.; Duvauchelle, N.; Vijayakrishnan, V.; Elhsissen, K. T. *J. Mater. Chem.* **1996**, *6*, 573.
26. Kim, D.; Jeong, S.; Moon, J. H. *Nanotechnology* **2006**, *17*, 4019.
27. Kheybari, S.; Samadi, N.; Hosseini, S. V.; Fazeli, A.; Fazeli, M. R. *DARU* **2010**, *18*, 3.
28. Soroushian, B.; Lampre, I.; Belloni, J.; Mostafavi, M. *Radiat. Phys. Chem.* **2005**, *72*, 111.
29. Tsuji, M.; Matsumoto, K.; Jiang, P.; Matsuo, R.; Tang, X.; Kamarudin, K. *Colloids Surf. A* **2008**, *316*, 266.
30. Jacob, J. A.; Mahal, H. S.; Biswas, N.; Mukerjee, T.; Kappor, S. *Langmuir* **2008**, *24*, 528.
31. Liu, P.; Zhao, M. *Appl. Surf. Sci.* **2009**, *255*, 3989.
32. Tominaga, M.; Shimazoe, T.; Nagashima, M.; Kusuda, H.; Kubo, A.; Kuwahara, Y.; Taniguchi, I. *J. Electroanal. Chem.* **2006**, *590*, 37.
33. Sanghi, R.; Verma, P. *Bioresour. Technol.* **2009**, *100*(1), 501.
34. Dastjerdi, R.; Montazer, M. *Colloids Surf. B* **2010**, *79*, 5.
35. Montazer, M.; Behzadnia, A.; Pakdel, E.; Rahimi, M. K.; Bameni Moghadam, M. *J. Photochem. Photobiol. B* **2011**, *103*, 207.
36. Guin, D.; Manorama, S. V.; Latha, J. V. M.; Singh, S. *J. Phys. Chem. C* **2007**, *111*, 13393.
37. Dastjerdi, R.; Montazer, M.; Shahsavan, S. *Colloids Surf. B* **2010**, *81*, 32.
38. Dastjerdi, R.; Montazer, M. *Colloids Surf. B* **2011**, *88*, 381.
39. Hashemizad, S.; Montazer, M.; Rashidi, A. *J. Appl. Polym. Sci.* **2012**, *125*, 1176.
40. Alisch-Mark, M.; Herrmann, A. *Biotechnol. Lett.* **2006**, *28*, 681.
41. Montazer, M.; Jolaei, M. *J. Appl. Polym. Sci.* **2010**, *116*, 210.
42. Montazer, M.; Jolaei, M. *J. Text. Inst.* **2010**, *101*, 165.
43. Tavanai, A. *J. Text. Inst.* **2009**, *100*, 633.
44. Montazer, M.; Sadighi, A. *J. Appl. Polym. Sci.* **2006**, *100*, 5049.

45. Bagherzadeh, R.; Montazer, M.; Latifi, M.; Sheikhzadeh, M.; Sattari, M. *Fiber Polym.* **2007**, *8*, 386.
46. Borchert, H.; Shevchenko, E. V.; Robert, A.; Mekis, I.; Kornowski, A.; Grübel, G.; Weller, H. *Langmuir* **2005**, *21*, 1931.
47. Ancutienė, K.; Strazdienė, E.; Nesterova, A. *Mater. Sci.* **2010**, *16*(4), 346.
48. Haghighat Kish, M.; Nouri, M. *J. Appl. Polym. Sci.* **1999**, *72*, 631.
49. Niu, S.; Wakida, T.; Shinji, O.; Hitoshi, F.; Shoji, T. *Text. Res. J.* **1995**, *65*, 771.
50. Pavia, D.; Lampman, M.; Kriz, G., Eds. Introduction to Spectroscopy: A Guide for Students of Organic Chemistry, 2nd ed.; Department of Chemistry, Western Washington University: Washington, **1996**, Chapter 2, p 50.
51. Popa, M.; Pradell, T.; Crespo, D.; Calderón Moreno, J. M. *Colloids Surf. A* **2007**, *303*, 184.
52. Socaciu, L. D.; Hagen, J.; Heiz, U.; Bernhardt, T. M.; Leisner, T.; Woste, L. *Chem. Phys. Lett.* **2001**, *340*, 282.
53. Sakthivel, S.; Neppolian, B.; Shankar, M. V.; Arabindoo, B.; Palanichamy, M.; Murugesan, V. *Solar Energy Mater. Solar Cells* **2003**, *77*, 65.
54. Rafey, A.; Shrivastava, K. B. L.; Iqbal, S. A.; Khan, Z. *J. Colloid Interface Sci.* **2011**, *354*, 190.
55. Wiley, B.; Sun, Y.; Mayers, B.; Xia, Y. *Chem. Eur. J.* **2005**, *11*, 454.
56. Luo, S.; Wang, F.; Shi, Z. *J. Sol-Gel Sci. Technol.* **2009**, *52*, 1.
57. Dastjerdi, R.; Montazer, M.; Shahsavan, S. *Colloids Surf. A* **2009**, *345*, 202.
58. Babaahmadi, V.; Montazer, M.; Toliyat, T.; Ghanbarafjeh, M. *Nanomater. Appl. Properties* **2011**, *1*, 183.
59. Montazer, M.; Rangchi, F. *Tekstil ve Konfeksiyon* **2009**, *2*, 128.